Evaluating ResNet-Based Self-Explanatory Models for Breast Lesion Classification

Adél Bajcsi[a], Camelia Chira[b] and Annamária Szenkovits[c]
Babeș–Bolyai University, Cluj-Napoca, Cluj, Romania
{adel.bajcsi, camelia.chira, annamaria.szenkovits}@ubbcluj.ro

Keywords: Breast Lesion Classification, ResNet-50, Self-Explanatory Models, Mammogram Analysis.

Abstract: Breast cancer is one of the leading causes of mortality among women diagnosed with cancer. In recent years, numerous computer-aided diagnosis (CAD) systems have been proposed for the classification of breast lesions. This study investigates self-explanatory deep learning models, namely BagNet and ProtoPNet, for the classification of breast abnormalities. Our aim is to train models to distinguish between benign and malignant lesions in breast tissue using publicly available datasets, namely MIAS and DDSM. The study provides a comprehensive numerical comparison of the two self-explanatory models and their respective backbones, as well as a visual evaluation of model performance. The results indicate that, while the backbone (black-box model) exhibits slightly better performance, it does so at the expense of interpretability. Conversely, BagNet, despite being a simpler model, achieves results comparable to those of ProtoPNet. In addition, transfer learning and data augmentation techniques are employed to enhance the performance of the CAD system.

1 INTRODUCTION

Breast cancer is one of the leading causes of death among women suffering from cancer. According to statistics of the (World Health Organization, 2024), breast cancer accounted for 2.3 million new cases and 666 000 deaths, making up 23.8% of all cancer diagnoses and 15.4% of cancer-related deaths worldwide.

Early stage cancer can be effectively treated with radiation therapy, chemotherapy, or surgery. Hence, in recent years, there have been numerous proposals for computer-aided diagnosis and detection systems (CAD) with the aim of helping the work of radiologists. Mammography is a frequently used, non-invasive method for breast cancer screening by doctors and scientists.

Both classical machine learning methods and modern deep learning techniques have been shown to provide promising results in medical imaging-based classification of breast lesions. Classical machine learning methods are easier to train, whereas deep learning models often achieve higher accuracy. Conversely, traditional machine learning algorithms are typically self-explanatory, whereas deep learning models lack interpretability, which is crucial for breast lesion classification. The challenges of automated medical imaging-based breast cancer diagnosis arise from (1) the lack of training samples, (2) the large variety of lesions in term of shape, size and appearance, and (3) the imbalance of class samples.

In general, training a deep neural network model involves a substantial amount of data due to the large number of parameters that must be optimized during the training process. Deep learning models often contain millions of parameters, and insufficient training samples with limited variance can lead to improper parameter optimization, resulting in overfitting. Medical datasets usually contain a few thousand records (at most) due to the limited number of subjects and data privacy concerns. Consequently, data augmentation has emerged as a crucial technique to artificially expand the size and variance of these datasets. By applying carefully selected transformations, data augmentation can increase the diversity and quantity of training samples without altering the essential characteristics of the data, thus improving the robustness and generalizability of the model.

There are critical fields where models are not allowed to make mistakes, including healthcare. Therefore, the interpretability and self-explainability of machine learning models are crucial for building trust and facilitating clinical adoption. Medical professionals need to understand how and why a model makes

[a] https://orcid.org/0009-0007-9620-8584
[b] https://orcid.org/0000-0002-1949-1298
[c] https://orcid.org/0009-0001-8579-6962

Bajcsi, A., Chira, C. and Szenkovits, A.
Evaluating ResNet-Based Self-Explanatory Models for Breast Lesion Classification.
DOI: 10.5220/0013121900003890

In *Proceedings of the 17th International Conference on Agents and Artificial Intelligence (ICAART 2025) - Volume 3*, pages 288-295
ISBN: 978-989-758-737-5; ISSN: 2184-433X

specific predictions to confidently integrate these tools into their decision-making processes. Clear explanations allow clinicians to verify and validate the results. Deep learning models are also known as black-box models. Hence, explainable deep learning models are being more and more researched.

In the current study, we investigate two explainable models, namely ProtoPNet (Chen et al., 2018) and BagNet (Brendel and Bethge, 2019). ProtoPNet is one of the first prototype-based, self-explanatory models introduced. On the other hand, BagNet converts ResNet-50 into an explainable model by incorporating the concept of bag-of-local features. Despite its simplicity, BagNet achieves high performance (Hesse et al., 2023). We aim to train models capable of distinguishing benign and malignant lesions in breast tissue using publicly available data sets of MIAS (Suckling et al., 1994) and DDSM (Heath et al., 1998; Heath et al., 2001). For easier comparability, we choose to build both ProtoPNet and BagNet on top of a ResNet-50 (He et al., 2015) black-box model. The study contains a comprehensive numerical comparison of the two explainable models and their backbone, as well as a visual evaluation of the performance of the model. The results show that BagNet has slightly better performance (93.25% on MIAS and 95.25% on DDSM) compared to ProtoPNet (78.11% on MIAS and 91.23% on DDSM). However, in terms of explainability, ProtoPNet can give more details on its predictions.

The rest of the paper is structured as follows: Section 2 offers an overview of state-of-the-art deep learning models for breast tumor classification. In Section 3 the proposed models are detailed. Next, Section 4 presents the data and setup used followed by a numerical and visual evaluation of the models. Finally, in Section 5 we state the conclusions and define future directions.

2 RELATED WORK

Early detection of tumors is essential to decrease the mortality caused by the specific type of cancer. In the literature, numerous machine learning-based CAD systems have been proposed for the classification of breast lesions. The current work focuses on distinguishing abnormalities extracted from digital mammograms. In the following paragraphs, key studies will be highlighted from the field of breast cancer classification with emphasis on interpretable models.

Supervised image classification by machine learning can be divided into two main subcategories: (1) traditional machine learning (ML) and (2) deep learning (DL). (Houssein et al., 2021; Hassan et al., 2022) provide a comprehensive reviews of breast cancer classification using various approaches. (Hassan et al., 2022) includes a study proposing the use of the discrete wavelet transform to extract features from images and classified using support vector machines (SVM). The proposed approach achieved 88.75% sensitivity on 75 mammograms from MIAS (Suckling et al., 1994). Another approach included in (Hassan et al., 2022) ((Suhail et al., 2018)) combined scalable Linear Discriminant Analysis (LDA) algorithms to extract the features and reduce the dimensionality, using five different classifiers, including SVM, Decision Tree (DT) and k-Nearest Neighbors (kNN). From the listed classification methods, DT achieved the best performance with 97.5% accuracy (SVM – 96%, kNN – 97.2%). In (Bajcsi and Chira, 2023) the classification performance of the features extracted from the Gray-Level Run-Length Matrices (GLRLM) is compared to the features extracted from the shape of the lesion. Using tree-based classifiers, (Bajcsi and Chira, 2023) concluded that shape features outperform texture features. (Bajcsi et al., 2024) proposed the combination of the extracted contour features and achieved 96.12% accuracy using the random forest (RF) classification algorithm on images from DDSM (Heath et al., 1998; Heath et al., 2001).

The advantage of a deep learning-based CAD system is that it can learn more complex patterns. Among the works reviewed in (Hassan et al., 2022), we highlight (Ansar et al., 2020) proposing a modified MobileNet that achieves an accuracy of 86.8% on DDSM (Heath et al., 1998; Heath et al., 2001) and 74.5% on CBIS-DDSM (Sawyer-Lee et al., 2016). ResNet-50 and Inception-V2 achieved 95.8% and 97.5%, respectively, on DDSM (Heath et al., 1998; Heath et al., 2001) as presented in (Houssein et al., 2021).

(Ragab et al., 2021) proposed the combination of deep learning and traditional machine learning. Deep learning like AlexNet, GoogLeNet, ResNet-18, ResNet-50, and ResNet-101 is used as input for SVM classifiers. The performance achieved is comparable to other approaches, reaching 97.4% accuracy on MIAS (Suckling et al., 1994).

Compared to traditional machine learning, deep learning models have more hyperparameters and need a great amount of data for training. However, several studies (Alruwaili and Gouda, 2022; Alkhaleefah et al., 2020; Ragab et al., 2021; Ansar et al., 2020) showed that transfer learning can improve the learning process of deep learning models. (Alruwaili and Gouda, 2022) compared the performance of ResNet-50 and NASNet using transfer learning on MIAS (Suckling et al., 1994) and reported 89.5% and

70%, respectively. In (Houssein et al., 2021) a novel deep convolutional neural network is proposed. The model is first trained on ImageNet (Deng et al., 2009), then fine-tuned on DDSM (Heath et al., 1998; Heath et al., 2001) achieving 89.9% sensitivity.

(Alkhaleefah et al., 2020) proposed the combination of transfer learning and data augmentation, in order to increase the performance of breast lesion classification models. (Alkhaleefah et al., 2020) reported a 20% increase in the test accuracy. In (Alkhaleefah et al., 2020), a VGG-19 model is fine-tuned on CBIS-DDSM (Sawyer-Lee et al., 2016) with 73.54% and 90.38%, with and without augmentation, respectively. The augmentations used were carefully selected to enhance the diversity of the training data while preserving the critical diagnostic features of the mammograms, ensuring that the integrity of the images remained intact. (Alkhaleefah et al., 2020) proposed the use of rotation, flipping, zooming, adjusting contrast, and brightness.

The interpretability and explainability of deep learning models in medical image classification are crucial to gain clinical trust, as they allow healthcare professionals to understand, verify, and validate the model's decisions, ensuring the safety and reliability of the diagnostic process. There are a limited number of proposals (Moroz-Dubenco et al., NA; Carloni et al., 2023; Balve and Hendrix, 2024) toward interpretable mammogram classification systems. Hence, our interest is to compare the performance of interpretable models for the classification of lesions. Moroz et al. (Moroz-Dubenco et al., NA) proposed a classical ML system achieving 95% test accuracy on a subset of the MIAS database (Suckling et al., 1994). (Carloni et al., 2023) investigate the applicability of ProtoPNet (Chen et al., 2018) self-explanatory model on CBIS-DDSM (Sawyer-Lee et al., 2016) and report 68.5% test accuracy. (Balve and Hendrix, 2024) proposed the application of post hoc techniques to generate heatmaps for the prediction of a CNN model. The authors included Grad-CAM, LIME, and Kernel SHAP methods. The best performance was 77% accuracy on MIAS (Suckling et al., 1994). (Balve and Hendrix, 2024) concluded that the Grad-CAM method outperformed the other methods in terms of time and explanation.

Based on a survey by (Rudin et al., 2022), explainable deep learning modes can be categorized as (1) post hoc and (2) self-explanatory models. Post hoc interpretability consists of algorithms that aim to generate an explanation for the prediction of an already trained model. These methods do not alter the model, but provide information on how the model makes decisions. On the other hand, the design of self-explanatory models is inherently interpretable. These models have built-in structures or mechanisms that allow them to provide explanations for their predictions. In this paper, we focus on self-explanatory models. BagNet and ProtoPNet generate explanations for their decision-making during training, as explained in (Rudin et al., 2022).

Based on previous research, in the present study, explainable deep learning models are investigated for the classification of breast lesion. Furthermore, transfer learning and data augmentation is applied to increase the performance of the CAD system.

3 PROPOSED APPROACH

The purpose of the current study is to distinguish benign and malignant lesions on mammograms using self-explanatory deep convolutional networks. The system starts with a preprocessing, followed by the decision-making model. In the next paragraphs, the aforementioned steps are detailed.

3.1 Preprocessing

Mammography is a commonly used method for the screening for breast cancer by doctors and machine learning methods as well. As a first step, the proposed system crops the lesions from the image using a bounding box. The bounding box is defined using a predefined segmentation mask of the lesion and is selected to be 25 pixels higher to enclose some of the surrounding area of the tumor. Malignant lesions, for example, have blurred boundaries. Hence, the tissues surrounding them can also contain useful information.

Breast abnormalities can appear in different shapes, sizes, and density. Image normalization is applied on the data to have 0 mean and 1 standard deviation. Normalization improves the convergence speed and stability of the training process by ensuring that the input data has a standardized scale, which helps to mitigate issues related to vanishing and exploding gradients. In addition, normalization contributes to a more consistent data distribution, ensuring that all input features contribute equally to the learning process. For normalization, the selected dataset's mean and standard deviation is defined and used. Finally, to overcome the size differences, the images are resized to 224×224.

3.2 Classification

In healthcare, transparency in decision making is essential. Therefore, we sought explainable models and selected two models based on ResNet-50 (BagNet (Brendel and Bethge, 2019) and ProtoPNet (Chen et al., 2018)) due to their promising results achieved in other fields (Galiger and Bodó, 2023; Hesse et al., 2023; Carloni et al., 2023).

ResNet-50 (He et al., 2015) is a widely used model for image classification. It overcomes the problem of vanishing gradients by introducing skip connections to bypass a given number of layers, allowing the gradient to flow directly through the network. To train the ResNet-50 model, we introduce four convolutions (add-on layers) before the final classification with batch normalization and dropout between, as proposed in (Chen et al., 2019). In the following subsections, we present the two explainable models.

3.2.1 BagNet

BagNet, proposed in (Brendel and Bethge, 2019), applies the bag-of-features concept to neural networks for image classification. The model classifies an image based on the occurrences of small local image features (defined by a receptive field) without taking into account their spatial ordering. BagNet modifies the ResNet-50 model as follows: (1) the initial 7×7 convolution is replaced by a 3×3 convolution, and (2) the number of 3×3 convolutions is decreased by leaving only the first bottleneck block of a residual block 3×3 convolution, and the rest is decreased to 1×1 convolutions.

(Brendel and Bethge, 2019) introduced three models named BagNet-q, where $q \in \{9, 17, 33\}$ represents the size of the receptive field. With a larger receptive field, the number of 3×3 convolutions increases. For every receptive field q the number of residual blocks starting with 3×3 convolution is 2, 3, 4, respectively, for every value q.

The model is able to explain its decision by generating detailed activation heatmaps, which visually highlight the individual pixels within the image that most strongly influenced the model's predictions. These heatmaps provide an intuitive and granular understanding of the decision-making process, allowing users to see exactly which regions of the image the model focused on.

3.2.2 ProtoPNet

Prototypical Part Network (i.e. ProtoPNet) was introduced by (Chen et al., 2018). ProtoPNet aims to bridge the gap between high-performance neural networks and the need for transparency. ProtoPNet operates by learning a set of prototypes that represent typical patterns or features seen in the training data. During classification, the model compares parts of the input image with these learned prototypes to determine the final prediction. This process allows the model to highlight specific regions of the mammogram that are similar to the learned prototypes, providing a visual explanation of why a particular classification was made. In the proposed approach, ResNet-50 is used to extract features from the input followed by the prototype layer, four convolution layers with batch normalization and dropout (Chen et al., 2019), and finally the classification layer.

4 EXPERIMENTAL RESULTS

In the present research, we performed experiments to compare two explainable deep learning models (BagNet (Brendel and Bethge, 2019) and ProtoPNet (Chen et al., 2018)) for the classification of breast abnormalities[1]. In the following subsections, we detail the datasets used and the setup of our experiments. We include a numerical and visual evaluation of the performance, and compare to other, state-of-the-art approaches.

4.1 Datasets

In the experiments, two publicly available datasets are utilized to evaluate the models' performance. Both datasets contain masks for the lesions, used to crop the region of interest. Detailed descriptions of these datasets are provided in the following.

4.1.1 MIAS

MIAS (Suckling et al., 1994) (Mammographic Image Analysis Society) is a small and frequently used dataset to train machine learning models on mammograms. MIAS contains 322 mammographies from 161 patients. Each patient has two images, one from each breast from the lateral view. From the total number of images, there are 115 breast tissues with abnormalities (62 benign, 51 malignant), 7 of them containing more than one lesion, with a total of 123 lesions. Due to their proximity to the margin, we excluded 10 tumors, leaving us with a total of 113 lesion images.

4.1.2 DDSM

DDSM (Heath et al., 1998; Heath et al., 2001) (Digital Database for Screening Mammography) is another

[1]The source code is available at: https://github.com/bajcsiadel/XAI-Mammogram-Classification/tree/ICAART-2025

dataset that is used frequently. It is a public collection with images from 1952 patients. The screening method resulted in four images: two images of each (left and right) breast from two perspectives (lateral and top). Of the total of 7808 mammograms, 4978 are classified as normal and 1402 as benign, and 1428 as malignant.

4.2 Data Augmentation and Transfer Learning

As mentioned in the previous section, the size of the dataset is very limited. In general, deep neural networks need large amount and diverse data to learn; otherwise, they are prone to overfitting. To overcome this issue, we use data augmentation (Alkhaleefah et al., 2020). Several affine transformations are used to increase the size of the dataset. Similarly to (Carloni et al., 2023), we employ (1) rotation $[-10°, 10°]$, (2) shear $[-10°, 10°]$, (3) perspective change (skew) 0.2, (4) horizontal and (5) vertical flip. Because the patches containing the tumor are extracted from the images, we can also apply flip operations on the images. Each transformation is applied ten times. In addition, a Gaussian noise is added to the resulting image with probability 0.15. This transformation mimics the noise from the mammography machine. As a result, the training data have increased 33 times (including the original image). To facilitate convergence and stability of the training process, every image is normalized as mentioned in Section 3.1. The abnormalities can differ in size. Therefore, the images are resized to 224×224.

As mentioned in Section 1, optimizing the model parameters with random initialization is time- and data-consuming. To overcome the issue, transfer learning (Alruwaili and Gouda, 2022) is applied. Transfer learning is a machine learning technique in which a model pre-trained on a large dataset is fine-tuned on a smaller, task-specific dataset. This approach leverages the knowledge acquired from initial training, often in a general domain such as ImageNet (Deng et al., 2009), to improve performance and accelerate training on the new task. In medical imaging, transfer learning is particularly valuable as it allows models to achieve high accuracy with limited labeled data, which is often a constraint in this field.

The models used are initialized with the weights of a model trained on ImageNet (Deng et al., 2009). However, ImageNet contains RGB (3-channel) images, and mammograms are grayscale (1-channel) images. In order to use such images as input, we slightly modify the weights of the first convolutional layer by summarizing the existing weights along the dimension of the channels.

4.3 Experimental Setup

The data used are divided into two sets without overlap, in 80% (train) - 20% (test) ration. To train the model, 5-fold cross-validation is used. This technique provides a more reliable estimate of how the model will perform on unseen data.

Medical datasets usually have an uneven distribution of classes. This could lead to biased predictions. This can result in a model that performs well on the majority class but poorly on the minority class, which is especially problematic in medical applications where accurate classification of rare conditions is critical. To address this problem, under-sampling is applied on the majority class in each fold.

In the following paragraphs, we detail the hyperparameters used for every model. To train the ResNet-50, cross-entropy (*CrossEnt*) loss and L_1 regularization is used with the Adam optimizer. Separate learning rates were specified to feature and add-on layer parameters 0.0001 and 0.003, respectively. In addition, to reduce training noise, a learning rate scheduler is applied that decreases the learning rate after every 5 epoch by 0.1. The batch size is maximized to 64 and train for 30 epochs.

For the training of BagNet models, we use cross-entropy (*CrossEnt*) loss with the SGD optimizer. The learning rate scheduler is applied, starting from 0.003 and decreasing by 0.8 after every 25 epoch. The batch size is set to 64, and trained for 50 epochs.

ProtoPNet being a slightly more complicated model, its loss function consists of three components: (1) cross-entropy, (2) clustering term with λ_1 weight – ensuring that an image of a class in the latent (feature) space is close to at least one patch of the same class – and (3) separation term with λ_2 weight – pushing the prototypes of different classes apart as presented in (Chen et al., 2018). To regularize training, we also add L_1 regularization with λ_3 weight. If a prototype is not the closest to any of the feature patches in its class, the cluster term will no longer have an impact on it. These prototypes will spread out and will become meaningless, yet promote the optimization of the separation cost. To solve this problem, we added L_2 regularization with λ_4 weight, penalizing the high norm of the computed prototypes. Based on preliminary experiments, the weights λ_1, λ_2, λ_3, and λ_4 in the loss term are set to 0.8, -0.08, 0.0001, and 0.01, respectively.

The training of ProtoPNet consists of three phases: (1) warm-up when the feature layer is

Table 1: Test performance (accuracy) of BagNet models using different receptive field.

	MIAS	DDSM
BagNet-9	0.8906 ± 0.0215	0.8781 ± 0.0223
BagNet-17	0.9325 ± 0.0258	0.9525 ± 0.0110

not trained (only the add-on, and prototype layers), (2) joint when the feature layer is also fine-tuned, and (3) fine-tune when only the classification layer is trained. Warm-up consists of 10 epochs with 256 batch size and a learning rate of 0.003 to optimize the parameters of the add-on layers and the prototype layer. The next phase (joint) is trained for 120 and 40 epochs, respectively on MIAS and DDSM, with 64 batch size (due to the increased number of parameters), the learning rate of feature, prototype and add-on layers parameters is set to 0.0001, 0.003 and 0.003, respectively. Moreover, learning rate scheduler is added with a step size of 30 and a degree of 0.1. The last layer (classification) is trained for 20 epochs, using a batch size of 256 and a learning rate of 0.0001. All phases utilize Adam optimizer.

4.4 Results

In our experiments, three models were trained to distinguish benign and malignant lesion: (1) ResNet-50, (2) BagNet and (3) ProtoPNet. First, we compare their numerical performance, followed by a visual evaluation of the interpretable models.

4.4.1 Numerical Results

As mentioned previously, 5-fold cross-validation was used during the training process. In the following, the mean and standard deviation of the resulting test accuracies will be presented.

ResNet-50 has proved to be a capable image classification model for general purposes. In the present experiments, the pre-trained model was fine-tuned to distinguish benign and malignant lesions. The test results on the MIAS and DDSM datasets show how the model can learn abnormalities of the breast tissue, achieving test accuracies 93.34% and 95.26%, respectively, for the datasets mentioned. In contrast, for high performance, the decision-making of ResNet-50 is not straightforward.

As mentioned in Section 3.2.1, BagNet has more versions based on the receptive field. In the current experiments, BagNet with receptive fields of 9 and 17 are used due to the small size of the lesions. The results achieved by the BagNet models are presented in Table 1. On both datasets, BagNet-17 outperforms BagNet-9 by 4% and 8%, respectively, on MIAS and DDSM.

Table 2: Test performance (accuracy) of ProtoPNet models with different number of prototypes per class trained.

protopypes per class	MIAS	DDSM
2	0.7182 ± 0.0725	0.9178 ± 0.0536
5	0.7811 ± 0.0614	0.9123 ± 0.0528
10	0.8168 ± 0.0422	0.8954 ± 0.0491

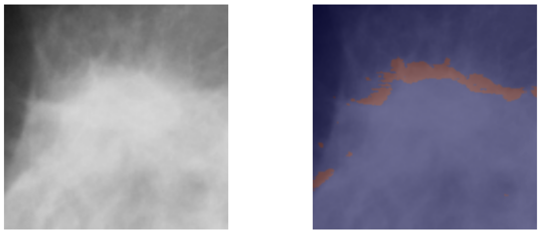

(a) Original images. (b) Heatmap.

Figure 1: Heatmaps generated by BagNet-17 for correctly classified malignant lesions from MIAS.

In case of ProtoPNet the number of learned prototypes can be adjusted based on the used images. In the experiments conducted, we investigated how the number of prototypes affects the classification performance. Based on the results shown in Table 2, we can conclude that with an increase in the number of prototypes, the test accuracy increases on a smaller variety dataset (MIAS); however, the accuracy decreases on a higher variety dataset (DDSM). On the other hand, for small variety datasets, the same characteristic is learned multiple times. Therefore, in the following, we report the results using 5 prototypes per class.

4.4.2 Visual Results

Both BagNet and ProtoPNet can generate explanations for their predictions. The main difference is that BagNet generates a single heatmap, while ProtoPNet can present the activation of every learned prototype on a given image. Fig. 1 shows a BagNet-17 generated heatmap for a correctly classified malignant image. Malignant lesions have obscure boundaries; therefore, it is reasonable for the model to focus on the margin of the abnormality.

On the other hand, the training process of the ProtoPNet involves the optimization of several prototypes per class. The advantage of these prototypes is that the model can learn different aspects of the classes. However, in the case of mammogram classification, this can also be a drawback due to the lack of data and the small variety of the images. Fig. 2 shows the activations generated by ProtoPNet. Notably, ProtoPNet also has prototypes of the malignant class that focus on the edge of the tumor.

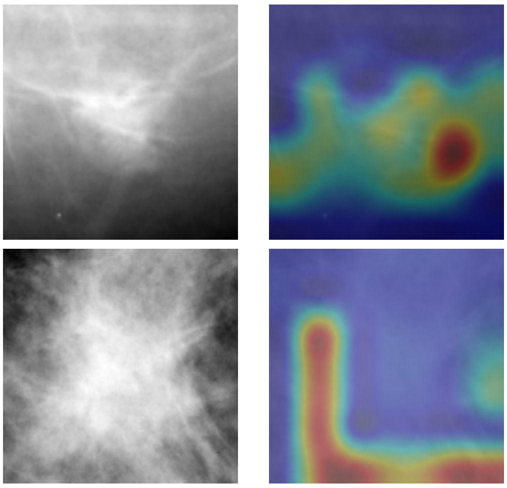

(a) Original images. (b) Prototype activation.

Figure 2: Most active prototype for classifying images as benign and malignant, respectively, using ProtoPNet.

Table 3: Test performance (accuracy) of the trained models in the experiment.

Network	MIAS	DDSM
ResNet-50	0.9338 ± 0.0059	0.9526 ± 0.0018
BagNet	0.9325 ± 0.0258	0.9525 ± 0.0110
ProtoPNet	0.7811 ± 0.0614	0.9123 ± 0.0528

4.5 Discussions

In the experiments carried out, self-explanatory models were trained to distinguish abnormalities in breast tissue. We investigated the applicability of two such models, namely ProtoPNet and BagNet, both of them using or based on ResNet-50 architecture. Table 3 summarizes the results previously presented.

The uninterpretable ResNet-50 had better performance in terms of accuracy than the two self-explanatory models, which had lower accuracy with approximately 1% (BagNet) and 15% (ProtoPNet). However, the reduced accuracy can be mitigated by the visual explanations offered by the models. This can be especially important for detecting error of bias in the models used.

Between the two explainable models, BagNet outperforms ProtoPNet in terms of performance on MIAS and DDSM. (Hesse et al., 2023) reported similar results when comparing the performance of BagNet and ProtoPNet. On the other hand, BagNet can provide a single explanation for its prediction, while ProtoPNet provides activation of several prototypes. There is a trade-off between interpretability and performance. In terms of complexity, BagNet is simpler (has fewer parameters compared to ProtoPNet) and therefore easier to train. Due to the lack of data, this could be a major concern. Furthermore, the results of ProtoPNet exhibit greater fluctuation compared to those of BagNet, which can be attributed to the increased difficulty in optimizing its parameters. This variability highlights the challenge of achieving consistent performance with more complex models in data-limited scenarios.

(Carloni et al., 2023) applied ProtoPNet on CBIS-DDSM (Sawyer-Lee et al., 2016) and reported the test accuracy of 68.5%. Compared to (Carloni et al., 2023), we introduced minor noise changes in the augmentation. However, the effect of the change in the augmentation must be further investigated on CBIS-DDMS for a better comparison.

Compared to the results of (Balve and Hendrix, 2024) both BagNet and ProtoPnet show better performance, with improvements of 15% and 1%, respectively, when trained on MIAS dataset. The difference in results can be attributed to the complexity of the models used. While (Balve and Hendrix, 2024) employed a simple CNN model, we used ResNet-50 as a base model for BagNet and ProtoPNet. Additionally, BagNet and ProtoPNet are inherently explainable, whereas the post-hoc methods used by (Balve and Hendrix, 2024) only attempt to generate explanations for the model's decisions.

Table 3 shows that indifferent from the model, the test results are better on DDSM than on MIAS. This can be explained by the size of the dataset and the increased variety of the data.

5 CONCLUSIONS AND FUTURE WORK

In the current study, the performance of two ResNet-50-based self-explanatory models (BagNet and ProtoPNet) is compared for the classification of breast lesions. Digital mammogram datasets are limited in size and image variety. To overcome this issue, transfer learning and image augmentation is applied. Our results show that BagNet outperforms ProtoPNet by achieving test accuracy of 93.25% and 95.25% on MIAS and DDSM, respectively, while ProtoPNet remains at 78.11% on MIAS and 91.23% on DDSM. As presented, the backbone achieves higher accuracy at the expense of explainability. Interpretability is an essential characteristic for models used in healthcare; hence, there is a critical need to balance accuracy with interpretability to ensure that clinical decisions are transparent and justifiable.

In future work, we will investigate other self-explanatory models, such as PIP-Net (Nauta et al., 2023). We will compare the performance of self-explanatory models with post hoc approaches applied on ResNet-50, evaluating both numerically and visually. In general, self-explanatory models are built on top of a black-box model, such as ResNet-50 in this paper. In future experiments, we will investigate the impact of the backbone on breast tumor classification. Moreover, to assess the system's interpretability, we will conduct user studies with domain experts.

REFERENCES

Alkhaleefah, M., Kumar Chittem, P., Achhannagari, V. P., Ma, S.-C., and Chang, Y.-L. (2020). The influence of image augmentation on breast lesion classification using transfer learning. In *2020 International Conference on Artificial Intelligence and Signal Processing (AISP)*, pages 1–5.

Alruwaili, M. and Gouda, W. (2022). Automated breast cancer detection models based on transfer learning. *Sensors*, 22(3).

Ansar, W., Shahid, A. R., Raza, B., and Dar, A. H. (2020). *Breast Cancer Detection and Localization Using MobileNet Based Transfer Learning for Mammograms*, page 11–21. Springer International Publishing.

Bajcsi, A., Andreica, A., and Chira, C. (2024). Significance of training images and feature extraction in lesion classification. In *Proceedings of the 16th International Conference on Agents and Artificial Intelligence - Volume 3: ICAART*, pages 117–124. INSTICC, SciTePress.

Bajcsi, A. and Chira, C. (2023). Textural and shape features for lesion classification in mammogram analysis. In *Hybrid Artificial Intelligent Systems*, pages 755–767. Springer Nature Switzerland.

Balve, A.-K. and Hendrix, P. (2024). Interpretable breast cancer classification using CNNs on mammographic images. .

Brendel, W. and Bethge, M. (2019). Approximating CNNs with bag-of-local-features models works surprisingly well on imagenet. *arXiv*.

Carloni, G., Berti, A., Iacconi, C., Pascali, M. A., and Colantonio, S. (2023). *On the Applicability of Prototypical Part Learning in Medical Images: Breast Masses Classification Using ProtoPNet*, pages 539–557. Springer Nature Switzerland, Cham.

Chen, C., Li, O., Tao, D., Barnett, A., Rudin, C., and Su, J. K. (2018). This looks like that: deep learning for interpretable image recognition. *Advances in neural information processing systems*, 32.

Chen, G., Chen, P., Shi, Y., Hsieh, C.-Y., Liao, B., and Zhang, S. (2019). Rethinking the usage of batch normalization and dropout in the training of deep neural networks.

Deng, J., Dong, W., Socher, R., Li, L.-J., Li, K., and Fei-Fei, L. (2009). Imagenet: A large-scale hierarchical image database. In *2009 IEEE Conference on Computer Vision and Pattern Recognition*, pages 248–255.

Galiger, G. and Bodó, Z. (2023). Explainable patch-level histopathology tissue type detection with bag-of-local-features models and data augmentation. *Acta Universitatis Sapientiae, Informatica*, 15(1):60–80.

Hassan, N. M., Hamad, S., and Mahar, K. (2022). Mammogram breast cancer CAD systems for mass detection and classification: a review. *Multimedia Tools and Applications*, 81(14):20043–20075.

He, K., Zhang, X., Ren, S., and Sun, J. (2015). Deep residual learning for image recognition. In *Proceedings of the IEEE Conference on Computer Vision and Pattern Recognition (CVPR)*, pages 770–778.

Heath, M., Bowyer, K., Kopans, D., Kegelmeyer, P., Moore, R., Chang, K., and Munishkumaran, S. (1998). *Current Status of the Digital Database for Screening Mammography*, pages 457–460. Springer Netherlands, Dordrecht.

Heath, M., Bowyer, K., Kopans, D., Moore, R., and Kegelmeyer, P. (2001). The digital database for screening mammography. In Yaffe, M., editor, *Proceedings of the Fifth International Workshop on Digital Mammography*, pages 212–218. Medical Physics Publishing.

Hesse, R., Schaub-Meyer, S., and Roth, S. (2023). Funnybirds: A synthetic vision dataset for a part-based analysis of explainable ai methods. In *Proceedings of the IEEE/CVF International Conference on Computer Vision (ICCV)*, pages 3981–3991.

Houssein, E. H., Emam, M. M., Ali, A. A., and Suganthan, P. N. (2021). Deep and machine learning techniques for medical imaging-based breast cancer: A comprehensive review. *Expert Systems with Applications*, 167:114161.

Moroz-Dubenco, C., Bajcsi, A., Andreica, A., and Chira, C. (N/A). Towards an interpretable breast cancer detection and diagnosis system. *Computers in Biology and Medicine*. Accepted.

Nauta, M., Schlötterer, J., van Keulen, M., and Seifert, C. (2023). PIP-Net: Patch-based intuitive prototypes for interpretable image classification. In *Proceedings of the IEEE/CVF Conference on Computer Vision and Pattern Recognition (CVPR)*, pages 2744–2753.

Ragab, D. A., Attallah, O., Sharkas, M., Ren, J., and Marshall, S. (2021). A framework for breast cancer classification using multi-DCNNs. *Computers in Biology and Medicine*, 131:104245.

Rudin, C., Chen, C., Chen, Z., Huang, H., Semenova, L., and Zhong, C. (2022). Interpretable machine learning: Fundamental principles and 10 grand challenges. *Statistics Surveys*, 16:1–85.

Sawyer-Lee, R., Gimenez, F., Hoogi, A., and Rubin, D. (2016). Curated breast imaging subset of digital database for screening mammography (cbis-ddsm)[skup podataka]. *The Cancer Imaging Archive*.

Suckling, J., Parker, J., and Dance, D. (1994). The mammographic image analysis society digital mammogram database. In *International Congress Series*, volume 1069, pages 375–378.

Suhail, Z., Denton, E. R. E., and Zwiggelaar, R. (2018). Classification of micro-calcification in mammograms using scalable linear fisher discriminant analysis. *Medical & Biological Engineering & Computing*, 56(8):1475–1485.

World Health Organization (2024). Cancer Today: Explore national indices, mortality, and prevalence for 36 cancer types in 185 countries. https://gco.iarc.fr/today/en. Accessed on 16/05/2024.